Study on Structures and Photoluminescence Emission of ZnS Microcrystals Grown by Thermal Deposition

Nguyen Van Nghia[1,2,*], Pham Thanh Huy[1], Le Van Vu[3], Nguyen Duy Hung[1]

[1]*Advanced Institute of Science and Technology (AIST),*
Hanoi University of Science and Technology (HUST), 01 Dai Co Viet, Hanoi, Vietnam
[2]*Thuy Loi University, 175 Tay Son, Dong Da, Hanoi, Vietnam*
[3]*Faculty of Physics, VNU University of Science, 334 Nguyen Trai, Hanoi, Vietnam*

Abstract: In this work, we report on the controlled synthesis of ZnS microstructures with high purity on Au-coated silicon substrates by thermal evaporation of ZnS powder in Ar gas ambient at atmospheric pressure. The growth mechanism is confirmed as a typical vapor–liquid–solid (VLS) process. The prepared ZnS microstructures have wurtzite (hexagonal) structures. The catalytically grown ZnS microstructures, including microwires and microbelts, are tens of micrometers in length. Energy-Dispersive X-Ray Spectroscopy EDS shows that the oxygen composition in the microstructures is trivial. The photoluminescence spectrum reveals strong ultraviolet emission and no other emission at room temperature also demonstrates that the ZnS microstructures are of high crystalline perfection. Optical transition from free exciton A, free exciton B are observed and analyzed through power-dependent at 10 K and temperature-dependent photoluminescence spectroscopy measurements are performed from 10 to 300 K. Our results indicate that ZnS microstructures grown by thermal evaporation, suggesting a great promise for high-efficiency light-emitting devices and lasers in the UV region.

Keywords: ZnS, microwires, microbelts, photoluminescence.

1. Introduction

Wide band-gap semiconducting nanowires and microwires have attracted considerable attention recently because of their promising applications in optoelectronics such as ultraviolet (UV) light sources (nanolasers, light emitting diodes), waveguides, photodetectors, sensor, phosphor host, optical coating, and solar cells [1-6]. Due to the wide band gap (3.68 eV for cubic phase and 3.70 eV for hexagonal-wurtzite phase at room temperature) and relatively large exciton binding energy (40 meV), ZnS is recognized as one of the most promising materials for a number of optoelectronic applications. Recently much effort has been devoted towards developing synthesis and characterization of one-

_____

dimensional ZnS nanostructures, such as nanowires, nanobelts, nanocables and nanotubes. Many techniques are used to synthesize ZnS such as thermal evaporation, hydrogen-assisted thermal evaporation, thermal chemical vapor deposition, hydrothermal synthesis route, solvothermal route, chemical vapor transport and condensation, electrodeposition-template,pulsed laser vaporization method [7-14]. However, it was difficult to get good optical properties of ZnS nanostructures from the products synthesized by the above mentioned methods. Their PL spectrum always presented UV emissions at 380 nm and visible range related to O impurities, Zn and S vacations, surface states, dislocations. To get high crystalline ZnS nanostructures their synthesis conditions are usually rigorous, such as high temperature and high pressure [14]. In this work, we report high quality crystal ZnS microstructures, strong UV emission from band to band transition, based on thermal evaporation method.

2. Experimental

The synthesis was performed in a conventional horizontal quartz tube furnace. The single crystal ZnS microstructures were synthesized on silicon substrates by thermal vapor deposition. A pure silicon (100) wafer was subjected to ultrasonic cleaning in ethanol for 30 min. Then, the wafer was treated with dilute HF (1 wt %) for 45 s and with deionized water and subsequently blow dried with nitrogen. High-purity ZnS (0.1 g, Aldrich, 99.99%), powders, which acted as the precursor materials, were placed into an alumina boat and positioned at the constant temperature zone of the horizontal tube furnace. The cleaned silicon substrates with size of 1 x 1.5 cm were placed in the low temperature zone at about 10 cm downstream from the aluminum boat and flow of argon, which acted as the carrier gas. A haft of the quartz tube of aluminum boat, silicon substrates was set up outside the tube furnace until the furnace was heated to deposition temperature. First, the quartz tube was pumped down to pressure of 1×10^{-3} Torr and heated to 600 $^{\circ}$C. After that, the high-purity argon was introduced into the tube and the mechanical rotary pump was turn off.The flow rates of Ar were controlled by a mass flow meter at 100 sccm. The temperature of the furnace was raised continually to growth temperature at a ramping rate of 10 $^{\circ}$C/min. To control ZnS microstructures, the substrate temperature is set at 1150 $^{\circ}$C and 1100 $^{\circ}$C, respectively. During synthesis the furnace temperature was maintained at growth temperature for 30 min, after that the furnace was allowed to cool naturally to room temperature. The morphology was examined by a field emission scanning electron microscopy (FESEM, JSM-7600F, Jeol). The composition was determined by the energy dispersive x-ray

spectroscopy (EDX, Oxford Instruments *X-Max* 50) attached to the FESEM. The phase structure, crystallinity and preferred orientation of as-synthesized ZnSwere characterized by an X-ray diffraction (XRD) (X-ray Siemens D5000) using Cu Kα radiation (λ=1.5406 Å) operated at 40 mA tube current.The XRD patterns were collected in the range of 20 $^{\circ}$ $\leq$ 2θ $\leq$ 70 $^{\circ}$ with a step of 0.05 $^{\circ}$ and collection time for each data point was set at 4 seconds. The emission spectra were recorded on a spectrophotometer (FHR1000, Horiba Jobin Yvon) equipped with a nanosecond pulsed Nd:YAG laser . The excitation wagelength is chosen at 266 nm.

3. Results and discussion

3.1. Morphology and structure of the microcrystals

FESEM were employed to study the morphology of the as-grown ZnS microstructures. Fig. 1 shows a series of preventative FESEM images of the ZnS microstructures grown on Au thin film

deposited Si substrates. Fig. 1(a) were taken on Au coated Si substrates annealed at 1100 ^{o}C, it is clearly seen that the Au particles have diameters around 50–100 nm. The products grown at 1150 ^{o}C on the Si substrate in Fig. 1 (b) show microbelts with 100–150 nm in thickness and tens of microns in lengths. When the substrate temperature decreases to 1000 ^{o}C, the morphologies of the products change from microbelts to microwires (Fig. 1(c)).
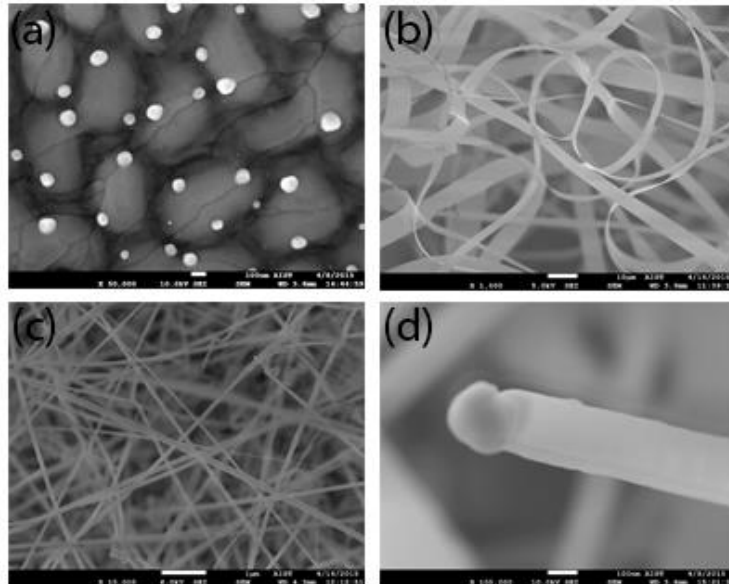

Figure1. FESEM images of Au nanoparticles on Si substrate
(a), ZnS microbelts (b), ZnS microwires (c) and ZnStip-end nanowire (d).
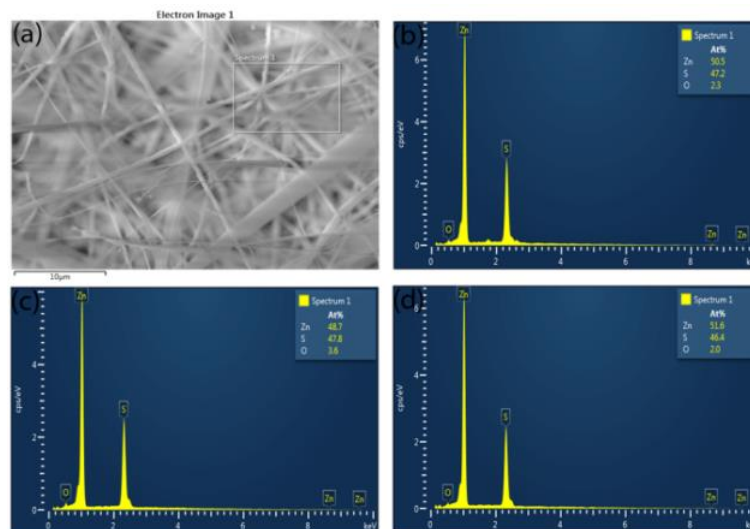

Figure2. The selected area EDS (a), EDS spectra of ZnS microbelts (b), microwires(c) and ZnS powder source.

A typical SEM image shows that ZnS microwires were formed in high density with 50–100 nm in widths and tens of microns in lengths. The width of microwires is similar to Au particle diameter. So

the growth mechanism of ZnS microwires is vapor-liquid-solid (VLS). These microwires are randomly oriented, and most of them are rather straight. To study the compositions of ZnS microstructures, the selected area EDS spectra were taken as shown in Fig. 2. EDXS spectra show that the microbelts and microwires contain Zn and S. The atom ratio of Zn and S is matched the stoichiometry quite well. Additionally, the O atom is noted that impurity in the microstructures was observed. To figure out the origin of O atom, the EDS spectrum of ZnS powder which used to deposit ZnS structures measured as shown in Fig. 2(d). This observations indicate that the ZnS powder contains O atom which may create the impurity in the microstructures.
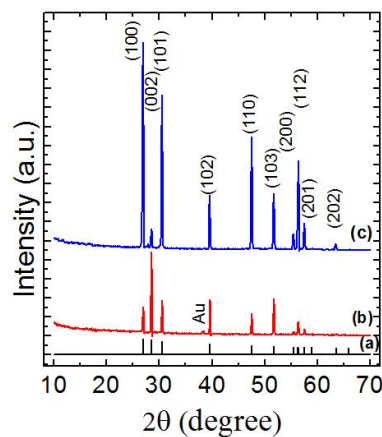

Figure 3. The JCPDS of No: 36-1450 (a) and XRD pattern of ZnS microwires (b) and microbelts (b) .

However, XRD patterns of all of the samples were almost identical with all the peaks representing the wurtzite phase of ZnS, which matches well in the JCPDS of No: 36-1450 with a good crystalline quality. and (200) planes of cubic Au, respectively can be indexed to a standard wurtzite-type hexagonal ZnS with the lattice constants of a = 0.382 nm and c = 0.6.26 nm . The products exhibit perfect phase purity; no ZnO phases are found.
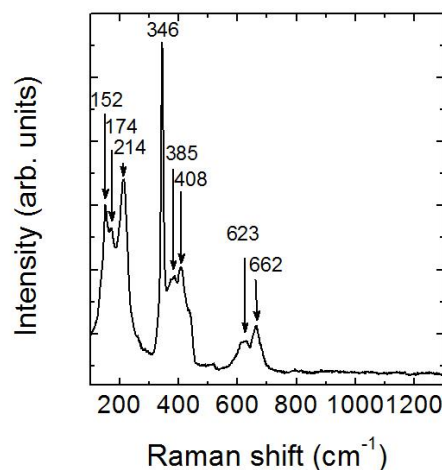

Figure 4. Raman spectra of ZnS microbelts.

Furthermore, Raman spectra (100–1300 cm^{-1}) of the ZnS microbelts were collected in air and at roomtemperature (Fig.4). Most peaks can be readily assigned tohexagonal ZnS crystalline [15, 16]. At low frequency, the peaks at 152 cm^{-1} and 174 cm^{-1} are assigned as disorder-activated second-order acoustic phonons [17, 18]. The possibility of observing these features from ZnS microbelts may be due to the surface enhancement effect promoted by the metal particles [19]. The peak centered at 214 cm^{-1} is assigned to a first-order LA mode. A strong scattering at 346 cm^{-1} is identified with A$_1$/E$_1$ of LO modes[19-22]. The scattering in the range 350–450 cm^{-1} is due to the combination of the TO + TA, LO + TA, LO + LA phonon modes [21]. The strongbroad Raman bands between 623 cm^{-1} and 662 cm^{-1} can be assigned to the TO + LA and 2LO modes [21]. The intensity ratio of the second-order LO to first-order LO phonon responses is closely relatedto the crystalline quality and/or exciton–LO phononcoupling strength [22].

3.2. Emission spectra of the microcrystals

Fig. 5 shows the PL spectra of the ZnS microbelts samples measured at room temperature. Fig 5(a) shows PL spectrum of ZnS microstructures under an average excitation density~ 142 W/cm^2. The ZnS microstructures spectra show only band to band emission at around 340 nm. Usually, ZnS nanostructure emissions are observed from band to band transition and the exciton combination and extrinsic defects in ZnS and ZnO [23-25]. However, only UV emission is observed in our work. The band edge photoluminescence of ZnS at room temperature was observed only in very high quality single crystals [25]. It could be assigned to the good crystal quality of grown ZnS microstructures.
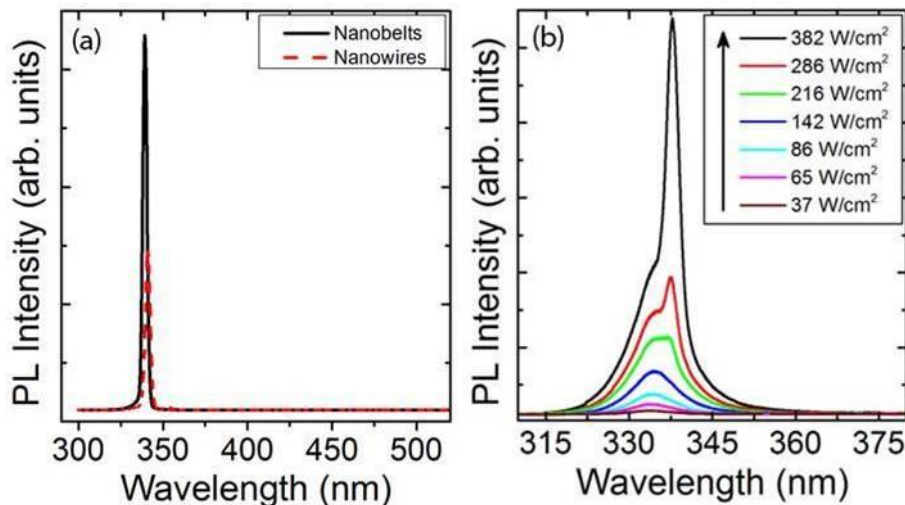

Figure 5. PL spectra of ZnS microstructuresat room temperature (a),
Power dependence of photoluminescenceat 10K (b).

To estimate the quality of ZnS microstructures, power dependence of PL of the microstructures at 10K was carried out, it is clearly seen the splitting energies of emission peak. At under an average excitation density~ 142 W/cm^2, UV emission peaks at 334 nm (~3.71 eV) dominates.When excitation density above 216 W/cm^2, another luminescence at 333.75 nm (~3.67 eV) appears. The energy difference of the two observed emissions are 40 meV can be assigned to free-exciton due to the spin-orbit interaction and crystal field splitting, the topmost valence band splits into two bands and the respective exciton states are denoted as free-exciton A and B [14, 26]. Fig. 6 shows temperature

dependence of PL of ZnS microstructures. It is clear from the figure that when the temperature increases, the intensity of peaks decreases and the peaks have a trend moving to long wagelength. Because integrated intensity is calculated by a fomular [27]:

$$I = \frac{I_0}{1 + A\exp(-E_\alpha / k_B T)}$$

Where I_0 is the integrated intensity at zero absolute temperature and A is a constant; E_α is activation energy. Therefore, the PL intensity decreases with increasing temperature. The reason why there is a transition of the peak position may be due to the band gap of semiconduction materials goes down when the temperature increases. Fig. 7 shows the integrated intendity at different temperatures of ZnS microstructures. PL yield of the ZnS microstructures at room temperature is as high as about 4% of that at 10 K.
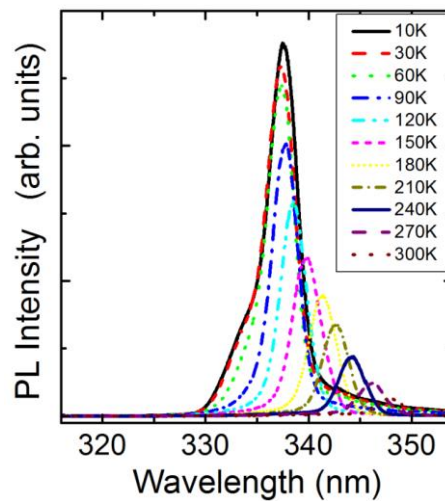

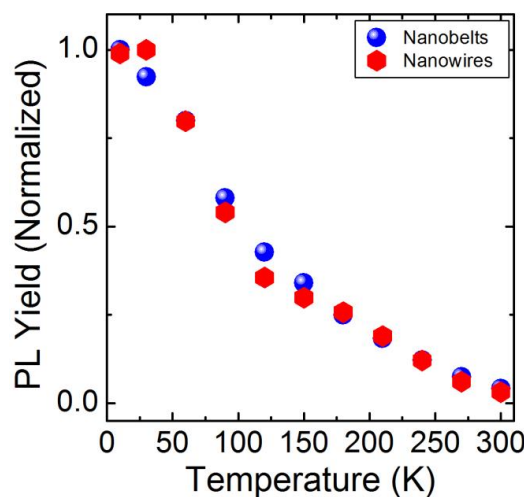Figure 6. Temperature dependence of PL of ZnS microstructures.

Figure 7. The integrated intensity of the spectra at different temperatures of ZnS microstructures.

4. Conclusions

In conclusion, we have synthesized high crystalline quality ZnS microstructures by the thermal evaporation method. FESEM, EDX and XRD were used to analyzethe morphology and composition. XRD showed that the ZnS microstructures have a wurtzite structure. The strong UV emission in the PL spectra of the ZnS microstructures and the observation of excitons in ZnS, which ensures good crystal quality of ZnS microstructures. Considering their lower density of crystalline defects and the sharp and narrow peak in UV region, ZnS microstructures can be envisaged as a potential material for technically important UV light emitter at microscale and nanoscale.

References

[1] J. C. Johnson, H. Q. Yan, P. D. Yang, and R. J. Saykally, Optical cavity effects in ZnO nanowire lasers and waveguides, J. Phys. Chem. B, vol. 107, no. 34, (2003), pp. 8816–8828.

[2] M. H. Huang, Room-Temperature Ultraviolet Nanowire Nanolasers, Science (80-.)., vol. 292, no. 5523, (2001), pp. 1897–1899.

[3] S. Chu et al., Electrically pumped waveguide lasing from ZnO nanowires., Nat. Nanotechnol., vol. 6, no. 8, (2011), pp. 506–510.

[4] W. Tian et al., Flexible ultraviolet photodetectors with broad photoresponse based on branched ZnS-ZnO heterostructure nanofilms, Adv. Mater., vol. 26, no. 19, (2014), pp. 3088–3093.

[5] Q. Shi, C. Wang, S. Li, Q. Wang, B. Zhang, and W. Wang, Enhancing blue luminescence from Ce-doped ZnO nanophosphor by Li doping, Nanoscale Res. Lett., vol. 9, no. 1, (2014), p. 410(1-7).

[6] J. Elias, R. Tena-Zaera, and C. Lévy-Clément, Effect of the Chemical Nature of the Anions on the Electrodeposition of ZnO Nanowire Arrays, J. Phys. Chem. C, vol. 112, no. 15, (2008), pp. 5736–5741.

[7] Q. Li and C. Wang, Fabrication of Zn/ZnS nanocable heterostructures by thermal reduction/ sulfidation, Appl. Phys. Lett., vol. 82, no. 9, (2003), pp. 1398–1400.

[8] Y. Jiang, X. M. Meng, J. Liu, Z. Y. Xie, C. S. Lee, and S. T. Lee, Hydrogen-assisted thermal evaporation synthesis of ZnS nanoribbons on a large scale, Adv. Mater., vol. 15, no. 4, (2003) pp. 323–327.

[9] J. S. McCloy and B. G. Potter, Photoluminescence in Chemical Vapor Deposited ZnS: Insight into electronic defects, Opt. Mater. Express, vol. 3, no. 9, (2013), pp. 1273–1278.

[10] G. H. Yue et al., Hydrothermal synthesis of single-crystal ZnS nanowires, Appl. Phys. A Mater. Sci. Process., vol. 84, no. 4, (2006), pp. 409–412.

[11] L. Chai, J. Du, S. Xiong, H. Li, Y. Zhu, and Y. Qian, Synthesis of wurtzite ZnS nanowire bundles using a solvothermal technique, J. Phys. Chem. C, vol. 111, no. 34, pp. 12658–12662, 2007.

[12] Q. Li and C. Wang, Fabrication of wurtzite ZnS nanobelts via simple thermal evaporation, Appl. Phys. Lett., vol. 83, no. 2, (2003), pp. 359–361.

[13] H. Y. Sun, X. H. Li, W. Li, F. Li, B. T. Liu, and X. Y. Zhang, Low-temperature synthesis of wurtzite ZnS single-crystal nanowire arrays, Nanotechnology, vol. 18, no. 11, (2007), p. 115604.

[14] Q. Xiong et al., Optical properties of rectangular cross-sectional ZnS nanowires, Nano Lett., vol. 4, no. 9, (2004), pp. 1663–1668.

[15] S. M. Scholz, R. Vacassy, L. Lemaire, J. Dutta, and Hofmann, Nanoporous Aggregates of ZnS Nanocrystallites, Appl. Organomet. Chem., vol. 12, (1998), pp. 327–335.

[16] M. Abdulkhadar and B. Thomas, Study of raman spectra of nanoparticles of CdS and ZnS, Nanostructured Mater., vol. 5, no. 3, (1995), pp. 289–298.

[17] H. W. Kim et al., One-step fabrication and characterization of silica-sheathed ITO nanowires, J. Solid State Chem., vol. 183, no. 10, (2010), pp. 2490–2495.

[18] D. Moore, J. R. Morber, R. L. Snyder, and Z. L. Wang, Growth of ultralong ZnS/SiO2 core-shell nanowires by volume and surface diffusion VLS process, J. Phys. Chem. C, vol. 112, no. 8, (2008), pp. 2895–2903.

[19] M. Lin, T. Sudhiranjan, C. Boothroyd, and K. P. Loh, Influence of Au catalyst on the growth of ZnS nanowires, Chem. Phys. Lett., vol. 400, no. 1–3, (2004), pp. 175–178.

[20] Q. Xiong, J. Wang, O. Reese, L. C. L. Y. Voon, and P. C. Eklund, Raman scattering from surface phonons in rectangular cross-sectional w-ZnS nanowires, Nano Lett., vol. 4, no. 10, (2004), pp. 1991–1996.

[21] J. H. Kim, H. Rho, J. Kim, Y. J. Choi, and J. G. Park, Raman spectroscopy of ZnS nanostructures, J. Raman Spectrosc., vol. 43, no. 7, (2012), pp. 906–910.

[22] Z.-G. Chen, L. Cheng, and J. Zou, Growth and optical properties of stacked-pyramid zinc sulfide architectures, CrystEngComm, vol. 13, no. 19, (2011), p. 5885.

[23] T. Tran, W. Park, and W. Tong, Photoluminescence properties of ZnS epilayers, J. Appl. …, vol. 81, no. 6, pp. 2803–2809, 1997.

[24] X. Fang et al., ZnS nanostructures: From synthesis to applications, Prog. Mater. Sci., vol. 56, no. 2, (2011), pp. 175–287.

[25] B. Y. Geng, X. W. Liu, Q. B. Du, X. W. Wei, and L. D. Zhang, Structure and optical properties of periodically twinned ZnS nanowires, Appl. Phys. Lett., vol. 88, no. 16, (2006), pp. 16–19.

[26] R. Chen et al., Optical and excitonic properties of crystalline zns nanowires: Toward efficient ultraviolet emission at room temperature, Nano Lett., vol. 10, no. 12, (2010), pp. 4956–4961.

[27] Ye CH, Fang XS, Wang M, and Zhang LD, Temperature-dependent photoluminescence from elemental sulfur species on ZnS nanobelts, J Appl Phys,99, (2006), 063504.